Proc. Natl. Acad. Sci. USA
Vol. 90, pp. 5959–5963, July 1993
Biophysics

A kinetic model for amyloid formation in the prion diseases: Importance of seeding

JON H. COME*, PAUL E. FRASER†, AND PETER T. LANSBURY, JR.*‡

*Department of Chemistry, Massachusetts Institute of Technology, Cambridge, MA 02139; and †Centre for Research in Neurodegenerative Diseases, University of Toronto, Toronto, ON Canada

Communicated by JoAnne Stubbe, February 26, 1993 (received for review November 6, 1992)

ABSTRACT **The transmissible spongiform encephalopathies (TSEs) are neurodegenerative diseases characterized by amyloid formation in the brain. The major amyloid protein is the prion protein (PrP). PrP and the β-amyloid protein of Alzheimer disease share a similar sequence that, in both cases, may be responsible for the initiation of protein aggregation *in vivo*. We report here that a peptide based on this sequence in PrP (PrP96–111M) forms amyloid fibrils. The existence of a kinetic barrier to amyloid formation by this peptide was demonstrated, suggesting that formation of an ordered nucleus is the rate-determining step for aggregation. Seeding was demonstrated to occur with PrP96–111M amyloid fibrils but not with amyloid fibrils of a related peptide. This effect is consistent with the proposal that the aggregation of PrP, which characterizes TSE, involves a nucleation event analogous to the seeding of a crystallization.**

Alzheimer disease (AD) (1) and the class of diseases known as the transmissible spongiform encephalopathies [TSEs; e.g., scrapie, Creutzfeldt–Jakob disease (CJD), and Gerstmann–Straussler–Scheinker disease (GSS)] (2, 3) are neurodegenerative diseases characterized by abnormal brain pathology and deposition of extracellular protein aggregate, often in the form of amyloid plaques (4). It was suggested that AD may be a type of TSE (5). However, the major plaque protein in AD is the β-amyloid protein (1), while in TSE the deposits consist primarily of the prion protein (PrP) (6). Scrapie can be transmitted via an infectious particle (prion), which appears to consist solely of an insoluble, protease-resistant form of PrP (PrP^{Sc}) (2). PrP^{Sc} appears to be chemically identical to its biosynthetic precursor, a neuronal cell-surface protein of unknown function, which has been designated PrP^{C} (3, 7). PrP^{Sc} may be an aggregate of PrP^{C}; however, the relationship between aggregation, amyloidogenesis, and infectivity is unclear (3, 6, 8–10). The brains of GSS patients contain amyloid fibrils composed of an 11-kDa fragment of PrP^{Sc} (11, 12), the sequence of which overlaps another amyloidogenic fragment of PrP^{Sc} (13–15). The discovery of this overlap led to the proposal that this 60-amino acid sequence may be sufficient for amyloid formation (11, 12).

A portion of the PrP sequence, including amino acids 96–111 (numbering from mature PrP; see Fig. 1), is highly conserved across species (6) and resembles the amyloidogenic C-terminal portion of the β-amyloid protein of AD (Fig. 1) (16). A nonpathogenic polymorphism occurs at amino acid 107 (codon 129) within this sequence and involves the conservative substitution of valine for methionine (17–19). The homozygous genotype seems to predispose to sporadic (19) and infectious (18) CJD. For example, 21/22 individuals with sporadic CJD were homozygous for methionine or valine at position 107, while the population in general is ≈50% homozygous (19).

We report here that two peptides based on the PrP sequence discussed above (PrP96–111M and PrP96–111V; see Fig. 1) form amyloid fibrils. Fibril formation follows a kinetic mechanism, which resembles crystallization—that is, nucleus formation is rate determining (20–24). The consequences of this kinetic mechanism for *in vivo* amyloidogenesis are discussed and a model that explains prion infectivity and the reported genotypic linkage to CJD is proposed.

MATERIALS AND METHODS

Search for Sequence Homology. The similarity between the β-amyloid protein of AD and PrP was discovered by a search of the sequence data base for hydrophobic sequences (hydropathy ≥ 1.4) of at least 12 amino acids that contain glycine residues at every fourth position. Proline residues were forbidden. Twenty-seven sequences with a high tendency to form β-sheet structure and a low tendency to form α-helical structure ($P_\beta - P_\alpha \geq 0.17$) were analyzed (25).

Peptide Synthesis, Purification, and Characterization. The peptides PrP96–111M, PrP96–111V, PrP96–111P, PrP96–111G, and Scr3 (see Fig. 1) were synthesized by standard 9-fluorenylmethoxycarbonyl (FMOC) chemistry on the 4-(2′,4′-dimethoxyphenyl-FMOC-aminomethyl)phenoxy resin and purified to homogeneity by reverse-phase HPLC (water/acetonitrile/0.1% trifluoroacetic acid). Purity of the peptides was determined to be >90% by analytical reverse-phase HPLC under isocratic conditions. Amino acid analysis and plasma desorption mass spectrometry (PDMS) analysis of each peptide were consistent with the desired product: PrP96–111M and Scr3, $(M + H)^+ = 1421$; PrP96–111V, $(M + H)^+ = 1389$; PrP96–111P, $(M + H)^+ = 1386$; PrP96–111G $(M + H)^+ = 1346$.

EM and Congo Red (CR) Staining. Samples for EM were prepared by stirring supersaturated solutions of peptide (250–350 μM) in 100 mM NaCl/8.2 mM Na_2HPO_4/1.8 mM NaH_2PO_4, pH 7.4 (hereafter referred to as the standard buffer) (see Fig. 3). EM samples were placed on carbon-coated copper grids, negatively stained with 2% uranyl acetate, and viewed at ×60,000 on a JEOL 1200 CX EM at 80 kV. Both peptides consistently stained with CR and exhibited birefringence when fibrils were formed in the presence of CR. Staining of preformed fibrils produced inconsistent results.

X-Ray Diffraction. Samples were prepared in hexafluoroisopropanol containing 10% formic acid (10 mg/ml) and slowly dried, under ambient conditions, in siliconized 0.7-mm-diameter thin-walled x-ray capillaries (Charles Suller

The publication costs of this article were defrayed in part by page charge payment. This article must therefore be hereby marked "*advertisement*" in accordance with 18 U.S.C. §1734 solely to indicate this fact.

Abbreviations: AD, Alzheimer disease; TSE, transmissible spongiform encephalopathy; CJD, Creutzfeldt–Jakob disease; PrP, prion protein; PDMS, plasma desorption mass spectrometry; CR, Congo red; FTIR, Fourier transform infrared spectroscopy; PrP^{Sc}, scrapie PrP; PrP^{C}, PrP^{Sc} precursor; PrP^{U}, unfolded form of PrP^{C}.

‡To whom reprint requests should be addressed.

Co., Natick, MA). Diffraction patterns were recorded on Kodak DEF film using double-mirror focused CuKα radiation generated by an Elliot GX-20 rotating anode (Marconi Avionics, Hertfordshire, U.K.) with a specimen-to-film distance of 72.2 mm. Exposure times were 1–2 days and reflections were measured as described (16).

Fourier-Transform Infrared Spectroscopy (FTIR). The peptide amyloid fibrils were centrifuged at 3000 rpm for 10 min and the solid was washed with water and dried onto CaF_2 plates and measured on a Perkin Elmer 1600 series FTIR.

Thermodynamic Solubility Measurement. A supersaturated solution of the peptide in standard buffer was stirred for 2–7 days. The suspension was then filtered through Millex-GV 0.22-μm aqueous filters (Millipore). Peptide concentration was determined by the BCA protein assay (Pierce) (26) using standards of the same peptide that had been previously calibrated by quantitative amino acid analysis.

Aggregation Kinetics and Seeding Experiments. Supersaturated solutions of the peptides were prepared in water by preparing a peptide film from hexafluoroisopropanol and then dissolving the film in water with brief agitation (2–3 mg/4 ml). Prolonged sonication caused the peptide to precipitate. This suspension was then filtered through a 0.22-μm filter, and protein concentration was measured by amino acid analysis or BCA protein assay. To initiate aggregation, a concentrated salt solution was added to produce a solution with a final concentration of 100 mM NaCl/10 mM phosphate/250–350 μM peptide, pH 7.4. Samples were agitated briefly (2–3 sec) prior to each turbidity measurement (400 nm). Seeding experiments were initiated by addition of 50 μl (5%) of the peptide suspension from a previous aggregation trial to a supersaturated peptide solution.

Coaggregation Experiments. Weighed mixtures of two peptides (PrP96–111M and Scr3 or PrP96–111V) in various ratios (90:10, 50:50, 10:90; 300 μM total peptide) were formulated. Aggregation was initiated as detailed above. After stirring for 2–7 days, the resulting suspension was filtered through 0.22-μm filters and the relative ratio of the two peptides in the soluble phase was determined by PDMS in the case of PrP96–111M/PrP96–111V mixtures and by reverse-phase HPLC in the case of PrP96–111M/Scr3 mixtures. Samples for PDMS were prepared by dissolving the peptides in hexafluoroisopropanol/water (2:1) and adsorbing them to nitrocellulose. The ratios were calculated from peak intensity or peak integration; both methods produced the same results. A correspondence between ratios determined by PDMS and ratios determined by other methods was found. Total peptide concentration was determined by BCA protein assay.

RESULTS

The β-Amyloid Protein from AD and the Amyloid Protein of TSE (PrP) Contain Similar Sequences. A 12-amino acid consensus sequence based on the critical C terminus of the amyloid protein of AD (16) was the basis of a search of the protein sequence data base. The consensus sequence emphasized the periodic occurrence (every 4th residue) of glycine residues within a hydrophobic background. Precedence was given to sequences rich in β-branched amino acids (valine, isoleucine). Of the 27 proteins containing sequences that met the criteria of the search, PrP was the only one that is known to form amyloid *in vivo*. A protein derived from the bacterial gene product OsmB also fits the search criteria (24). The homologous PrP sequence (residues 97–108) was included in the synthetic peptides PrP96–111M and PrP96–111V (Fig. 1). It must be noted that this sequence is sufficient, but not necessary, for amyloid formation (see below).

Model Peptides Based on the Similar Sequence Form Amyloid Fibrils. Five model peptides, based on the PrP-(96–111) sequence, were synthesized (Fig. 1). The peptides PrP96–111M and PrP96–111V were based on the two naturally occurring sequences. Peptides PrP96–111P and PrP96–111G were identical to the natural sequence except at position 107. The peptide Scr3, which has a composition identical to PrP96–111M but a permuted sequence, was designed to test the importance of the glycine periodicity.

β-protein of AD (25-42)	...GSNK GA I I GLMVGGVVIA-CO_2H
PrP (96-111):	.....AGAVVGGLGGY**M**LGSA... **V**
PrP96-111M:	AcHN-AGAVVGGLGGY**M**LGSA-$CONH_2$
PrP96-111V:	AcHN-AGAVVGGLGGY**V**LGSA-$CONH_2$
PrP96-111P:	AcHN-AGAVVGGLGGY**P**LGSA-$CONH_2$
PrP96-111G:	AcHN-AGAVVGGLGGY**G**LGSA-$CONH_2$
Scr3:	AcHN-AGAVGVLGGYGMLGSA-$CONH_2$

FIG. 1. A comparison of hydrophobic sequences from the β-amyloid protein of AD and the PrP. Model peptides discussed here are shown below (sequence differences are in boldface).

The peptides PrP96–111V, PrP96–111M, and Scr3 formed amyloid fibrils (visualized by EM), which stained with CR. The x-ray diffraction pattern of the PrP96–111M fibril is consistent with the β-fibril model of amyloid structure (27) (Fig. 2). The FTIR spectra of the PrP96–111M, PrP96–111V, and Scr3 fibrils were very similar and dominated by a low-frequency absorption amide I band (1630 cm^{-1}). This spectral feature is also prominent in the FTIR spectrum of naturally derived PrP27–30 (28).

Peptide Amyloid Formation Is Nucleation Dependent. The thermodynamic solubilities of PrP96–111M, PrP96–111V, and Scr3 were indistinguishable (15–25 μM), while PrP96–111P and PrP96–111G were significantly more soluble (>3 mM and 500 μM, respectively). Supersaturated solutions of the amyloidogenic peptides were metastable. Amyloid formation did not proceed immediately but after a defined time period or lag time. This behavior is reminiscent of crystal

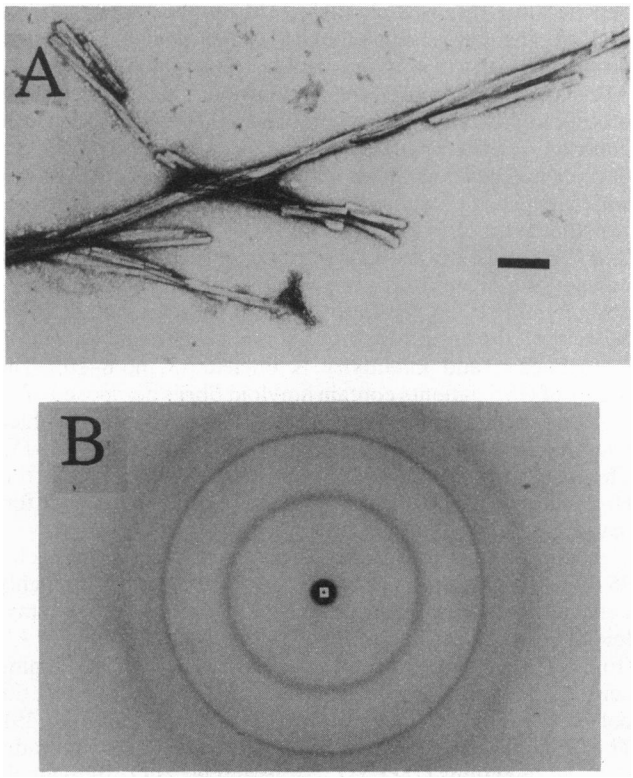

FIG. 2. (*A*) EM picture of PrP96–111M fibrils. (Bar = 1000 Å.) (*B*) X-ray diffraction pattern of unoriented PrP96–111M fibrils. Two major reflections were observed at 4.69 and at 7.5 Å, which may result from the interstrand and intersheet spacings, respectively, in a β-fibril (16, 27).

growth (20, 21, 23). Due to the sensitivity of nucleation to environmental factors and agitation, lag times were difficult to reproduce within better than ±20%.

Amyloid Formation Can Be Nucleated, or Seeded, by Peptide Fibrils. Analogous to the seeding of a crystallization, amyloid formation by the peptide PrP96–111M was seeded by addition of its own fibrils (Fig. 3) (24). In addition, fibrils of peptide PrP96–111V served as competent seeds. However, the fibrils of peptide Scr3 did not seed aggregation of PrP96–111M. Scr3 showed a similar selectivity; its aggregation was seeded by Scr3 fibrils but not fibrils of PrP96–111M.

Coaggregation of Peptide Models Show That the Met/Val Polymorphism May Not Be Distinguished at the Kinetic Level. To investigate the sequence specificity of amyloid formation at the kinetic level, a series of coaggregation experiments were performed in which supersaturated mixtures, equimolar in two peptides, were allowed to aggregate. In the case of Scr3/PrP96–111M mixtures (peptides that did not seed each other), 50:50 mixtures aggregated more slowly than did pure solutions of either peptide at the same total peptide concentration. In contrast, in the PrP96–111M/PrP96–111V case (peptides that seeded each other), no difference in aggregation rate was detected between 50:50 mixtures and pure solutions at the same total peptide concentration.

Coaggregation of Peptide Models Shows That the Met/Val Polymorphism Is Distinguished at the Thermodynamic Level. To study the sequence specificity of amyloid formation at the thermodynamic level, a similar series of coaggregation experiments were performed in which supersaturated mixtures of two peptides in various ratios were allowed to form amyloid. The ratio of the two peptides in the initial supersaturated solution was compared to the ratio of the two peptides in the soluble phase after aggregation (saturated solution). In the case of PrP96–111M and Scr3, the ratio in the saturated solution after 2–6 days was independent of that of the initial solution. The final supernatant was saturated in each peptide, indicating that PrP96–111M and Scr3 aggregate independently of one another. The identical experiment was performed with the peptides PrP96–111M and PrP96–111V

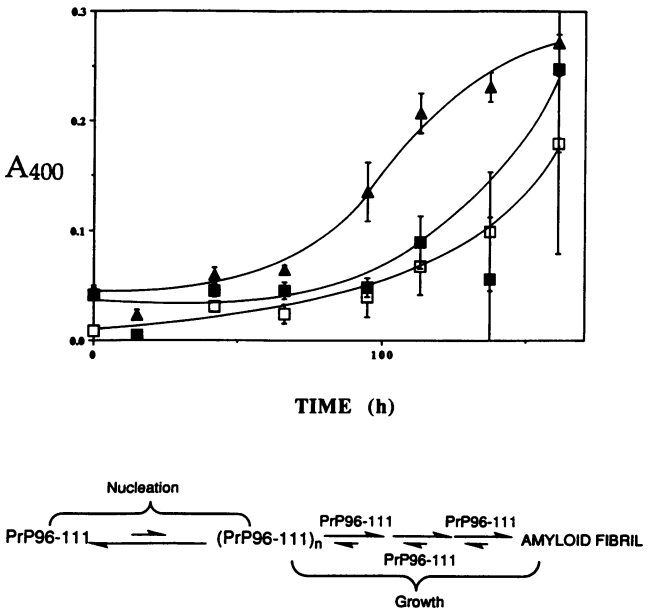

FIG. 3. (*Upper*) Aggregation of PrP96–111M as followed by turbidity measurements (400 nm). □, Unseeded PrP96–111M; ▲, PrP96–111M self-seeded; ■, PrP96–111M seeded with Scr3. PrP96–111V fibrils were also found to be capable of seeding amyloid formation. Each point represents average of triplicate runs. (*Lower*) Proposed kinetic scheme based on analogy to crystallization kinetics (23).

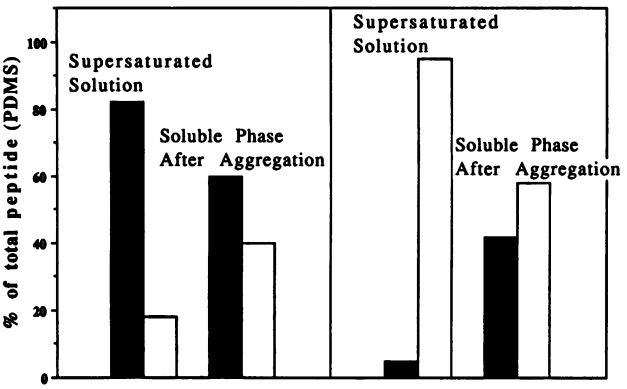

FIG. 4. Coaggregation of PrP96–111M (■) and PrP96–111V (□). Two experiments, differing in relative ratios of the two peptides in the initial supersaturated solution, are shown. Relative amounts of the two peptides in solution as determined by PDMS are shown. Left pair of bars in each panel, initial supersaturated solution (300 μM total peptide); right pair of bars in each panel, soluble phase after amyloid formation (2–7 days; 30 μM total peptide). Aliquots removed during aggregation indicated that the soluble phase slowly approaches an equilibrium mixture, which reflects the thermodynamic solubilities of the two peptides. Data are averages of six trials (error is ±8 units on *y* axis) with PrP96–111M and PrP96–111V; analogous results were obtained with PrP96–111M and Scr3.

(Fig. 4), which differ at a single amino acid and could not be distinguished at the kinetic level (see above). A similar result was obtained—that is, the composition of the saturated solution after 2–6 days was different than the composition of the initial supersaturated solution. Analysis of early time points in the process (data not shown) indicated that the peptide ratio was gradually approaching the equilibrium solubility ratio. The portion of soluble peptide represented by the minor component increased steadily during this time. The final total thermodynamic solubility of the mixture was greater than that of either pure peptide (30 μM vs. ≈20 μM). This result suggests that the Met-107 to Val (M107V) polymorphism, which may not be recognized at the kinetic level (nucleus formation) is distinguished at the thermodynamic level (amyloid formation).

DISCUSSION

We have discovered a similarity between a sequence at the C terminus of the β-amyloid protein, which is critical for amyloidogenesis (16), and a sequence in PrP. This similarity suggests a general mechanism of amyloid formation, which is supported by the results reported here. We propose that the PrP96–111 sequence is critical for formation of extracellular amyloid and for replication of the infective prion. Our results suggest a nucleation-dependent model for prion formation.

Synthetic peptides corresponding to PrP residues 96–111 (PrP96–111M and PrP96–111V; Fig. 1) were sparingly soluble and formed rigid, unbranched amyloid fibrils (EM, FTIR, CR staining, x-ray diffraction). A peptide with the same composition as PrP96–111M, but a permuted sequence (Scr3), formed similar amyloid fibrils, suggesting that the ability to form amyloid may characterize many sequences. The distinguishing factors are the rate of amyloid formation, the seeding of amyloid formation, and the stability (solubility) of the fibrils. Peptides with proline or glycine at position 107, replacing the natural Met/Val, were significantly more soluble than PrP96–111M and PrP96–111V.

The peptides PrP96–111M, PrP96–111V, and Scr3 showed a kinetic barrier to amyloid formation, which is also characteristic of crystal growth and suggests that the aggregate is ordered (Fig. 3) (2, 20–24). Supersaturated solutions of these peptides were stable for a period of days (we call this

phenomenon kinetic solubility), after which time aggregation proceeded until the thermodynamic solubility was attained. The thermodynamic and kinetic solubilities of a given peptide are not necessarily correlated. By analogy to crystal growth, we propose that the initial lag time represents the time required for formation of a nucleus, which initiates rapid growth of the fibril (Fig. 3) (2, 20, 21, 23). The nucleation-dependent mechanism of amyloid formation has several consequences, which may be relevant to amyloid formation *in vivo*. First, the rate of nucleus formation can be extremely sensitive to concentration, depending on the number of monomers involved (23). Second, endogenous materials could act as heterogeneous nucleators or nucleation inhibitors. For example, the dye CR, which has been shown to inhibit PrP^{Sc} formation in cell culture (29), inhibits nucleation of the peptide PrP96–111M *in vitro*.

Consistent with nucleation being the rate-determining step of amyloid formation, addition of peptide PrP96–111M or PrP96–111V amyloid fibrils to a supersaturated solution of PrP96–111M resulted in a substantial reduction of the lag time (Fig. 3) (20, 21, 23). In contrast, Scr3 fibrils were unable to nucleate precipitation of PrP96–111M, nor could PrP96–111M fibrils nucleate Scr3 precipitation (although both could self-nucleate)—possibly a consequence of subtle differences in fibril architecture caused by the altered glycine periodicity. This discrimination illustrates that specific interactions between hydrophobic residues are involved in amyloid formation.

Individuals who are homozygous at PrP position 107 are predisposed to sporadic and infectious CJD (17–19). To model the heterogeneous genotype, coaggregation of the PrP model peptides PrP96–111M and PrP96–111V was studied. Mixtures of PrP96–111M and PrP96–111V aggregated at rates comparable to pure solutions at the same concentrations, and these peptides seeded aggregation by each other. However, amyloid formation by the two peptides was independent at the thermodynamic level; that is, the mixed solutions were more soluble than the pure solutions. This behavior suggests that homogeneous amyloid is more stable than heterogeneous amyloid. We were unable to determine conclusively whether the mixed aggregate was formed transiently. The fact that Met-107 and Val-107 may not be distinguished at the kinetic level but are distinguished at the thermodynamic level *in vitro* may have implications for *in vivo* PrP amyloid formation. Homozygous individuals should rapidly form homogeneous amyloid characterized by stable interactions in the PrP96–111 region. However, under similar conditions, heterozygotes would form heterogeneous amyloid, which would be more susceptible to solubilization and clearance as it equilibrates to the more stable homogeneous amyloid. This postulate depends on the assumption that amyloid formation is reversible, which has been demonstrated for AD amyloid plaque (30).

A MODEL FOR PRION FORMATION AND REPLICATION

Repeated attempts to demonstrate a nucleic acid component of the infectious prion have failed (2, 3, 31–34). To reconcile the virus-like qualities of the prion with the fact that it apparently comprises a single protein, Griffith (32) proposed that PrP^{Sc} and PrP^{C} are conformational isomers. All subsequent models agree with that postulate; however, they differ with respect to the identity of the slow step (kinetic barrier)

Model	Aggregation State of PrP^{Sc}	Kinetic Barrier to Sporadic Disease	Role of PrP^{Sc}
1	monomer	conformational interconversion ($PrP^{C} \longrightarrow PrP^{Sc}$)	catalyst
2	oligomer	conformational interconversion	catalyst
3	oligomer	nucleation (see below)	SEED

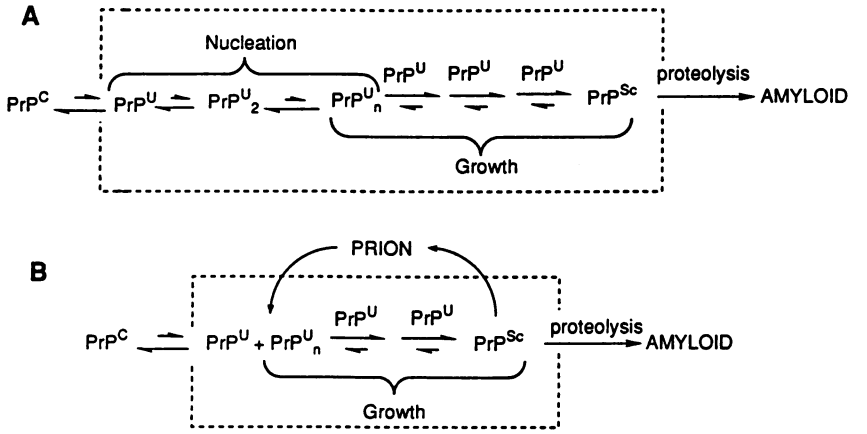

FIG. 5. (*Upper*) Table distinguishing the model for prion formation favored by the authors and supported by the experiments reported here (model 3) from other models of scrapie transmission. (*Lower*) Mechanism based on model 3 to explain PrP^{Sc} formation in sporadic (*A*) and infectious (*B*) TSEs. PrP^{Sc} refers to the protease-resistant form of a PrP aggregate, which may be the sole component of the prion (3, 33, 34). The aggregating monomer is a partially unfolded form of PrP^{C}, designated PrP^{U}, in which the hydrophobic sequence PrP-(96–111) is solvent exposed. Sporadic PrP^{Sc} formation (*A*) would be slow and dependent on the concentration of PrP^{U} (23). The unfolding equilibrium will depend on the environment (e.g., lysosomal pH may stabilize PrP^{U}) and could be sensitive to point mutations in PrP^{C} (35). The infectious prion (*B*) may contain aggregated PrP; the nucleus (PrP^{U}_{n}) could be derived from the prion. PrP^{Sc} and PrP^{U}_{n} may differ with respect to their physical properties (6, 36) as well as their molecular size. The formation of PrP^{Sc} in infectious TSE (*B*) may arise from the colocalization of the nucleus or seed (PrP^{U}_{n}) and the monomer (PrP^{U}) in the lysosome. In this case, the rate of formation of PrP^{Sc} would depend on the growth rate (nucleation is bypassed) and would therefore be much less sensitive to the concentration of PrP^{U} than the rate in *A*. Boxes indicate portion of proposed aggregation process modeled by experiments described here.

in sporadic disease, the aggregation state of the active component of the prion PrP^{Sc}, and the nature of PrP^{Sc} activity (Fig. 5).

One model (model 1) holds that conversion of PrP^{C} to PrP^{Sc} is very slow, consistent with the rare occurrence of sporadic prion disease. Infection would result from the fact that this conformational change could be catalyzed by PrP^{Sc} via heterodimer (PrP^{C}–PrP^{Sc}) formation (3, 32). PrP^{Sc} would rapidly aggregate to form the insoluble prion. This scenario accounts for replication and infectivity of the prion. However, there is no experimental evidence that directly supports this proposal, nor is there precedent for this type of process. Alternatively, the conformational change from PrP^{C} to PrP^{Sc} could be catalyzed by an aggregate of PrP^{Sc} rather than the monomer (model 2) (32). The aggregation of bacterial flagellin proceeds via this type of mechanism (37).

A third model, which we favor (model 3), is based on the nucleation-dependent mechanism of amyloid formation, which is demonstrated here (2, 32). This model assumes that PrP^{Sc} is an aggregate. The kinetic barrier to the conversion of PrP^{C} to PrP^{Sc} would be nucleation rather than conformational interconversion. Infection would involve the circumvention of this slow step by introduction of a seed that initiates aggregation. Seeding of amyloid formation is demonstrated here (24). The conformational interconversion from PrP^{C} to PrP^{Sc} may not require catalysis; we propose that PrP^{Sc} may be easily accessible from PrP^{C} or from an unfolded form of PrP^{C} (PrP^{U}; Fig. 5). This situation is precedented in protein self-assembly processes (38).

Peptides derived from PrP demonstrate aggregation kinetics consistent with model 3. We propose that the sequence PrP-(96–111) may initiate prion formation *in vivo* via a nucleation-dependent self-assembly mechanism (2). Since this hydrophobic sequence is unlikely to occur at the surface of PrP^{C}, the aggregating species may not be PrP^{C} but a partially unfolded form of PrP^{C} in which the 96–111 sequence is exposed (PrP^{U}; Fig. 5) (7, 21, 22). The peptides PrP96–111M and PrP96–111V are flexible models for PrP^{U}. Spontaneous aggregation of PrP^{U} would be expected to be very slow (Fig. 5*A*). The infectious prion may contain an aggregate of PrP^{U} (PrP^{Sc} or PrP^{U}_{n}; Fig. 5*B*) in which the hydrophobic PrP-(96–111) sequence is exposed and could serve as the template, or seed, for fibril growth (2, 31). Thus, infection may bypass the slow nucleation step by providing a seed for amyloid formation (Fig. 5*B*). Replication of infectivity could be explained by the fragmentation of fibrils, which would expose additional growth surfaces. Based on the model studies discussed here, we propose that deletion of the PrP-(96–111) sequence from PrP^{C} or introduction of the M107P point mutation could render mice resistant to infection (33).

CONCLUSION

In both AD and the prion diseases, extracellular amyloid plaques are found. In both cases, aggregation may result from the local concentration of a normal protein species (β protein or PrP) with an exposed hydrophobic sequence, leading to nucleation of amyloid formation. We have demonstrated that similar hydrophobic sequences may drive the aggregation process in these two diseases. Peptides based on these sequences suggest a kinetic model for amyloid formation and will eventually enable elucidation of the aggregation process at the molecular level (16, 39) and the discovery and design of inhibitory agents.

Note. After this work was completed, a paper appeared in which peptides based on several sequences in PrP were studied (40). It was reported that the peptides PrP91–98 (our numbering) and PrP91–105 formed amyloid fibrils. The peptide PrP99–114M did not form amyloid fibrils. No kinetic studies were reported.

We thank Prof. Charles Weissmann, Dr. Byron Caughey, and Prof. Jamie Williamson for helpful discussions. We thank Dr. Daniel Kirschner for use of his x-ray diffraction equipment. P.T.L. is the Firmenich Assistant Professor of Chemistry, a Sloan Research Fellow, and a Camille and Henry Dreyfus Teacher-Scholar.

1. Katzman, R. & Saitoh, T. (1991) *FASEB J.* **5**, 278–286.
2. Brown, P., Goldfarb, L. G. & Gajdusek, D. C. (1991) *Lancet* **337**, 1019–1022.
3. Prusiner, S. B. (1991) *Science* **252**, 1515–1522.
4. Prusiner, S. B., Groth, D. F., Bolton, D. C., Kent, S. B. & Hood, L. E. (1984) *Cell* **38**, 127–134.
5. Prusiner, S. B. (1984) *N. Engl. J. Med.* **310**, 661–663.
6. Stahl, N. & Prusiner, S. (1991) *FASEB J.* **5**, 2799–2806.
7. Caughey, B. & Raymond, G. J. (1991) *J. Biol. Chem.* **266**, 18217–18223.
8. Gabizon, R., McKinley, M. P., Groth, D. & Prusiner, S. B. (1988) *Proc. Natl. Acad. Sci. USA* **85**, 6617–6621.
9. Prusiner, S. B., Scott, M., Foster, D., Pan, K.-M., Groth, D., Mirenda, C., Torchia, M., Yang, S.-L., Serban, D., Carlson, G. A., Hoppe, P. C., Westaway, D. & DeArmond, S. J. (1990) *Cell* **63**, 673–686.
10. Xi, Y. G., Ingrosso, L., Ladogana, A., Masullo, C. & Pocchiari, M. (1992) *Nature (London)* **356**, 598–601.
11. Giaccone, G., Verga, L., Bugiani, O., Frangione, B., Serban, D., Prusiner, S. B., Farlow, M. R., Ghetti, B. & Tagliavini, F. (1992) *Proc. Natl. Acad. Sci. USA* **89**, 9349–9353.
12. Tagliavini, F., Prelli, F., Ghiso, J., Bugiani, O., Serban, D., Prusiner, S. B., Farlow, M. R., Ghetti, B. & Frangione, B. (1991) *EMBO J.* **10**, 513–519.
13. Prusiner, S. B. (1989) *Annu. Rev. Microbiol.* **43**, 345–374.
14. Prusiner, S. B., McKinley, M. P., Bowman, K. A., Bolton, D. C., Bendheim, P. E., Groth, D. F. & Glenner, G. G. (1983) *Cell* **35**, 349–358.
15. DeArmond, S. J., McKinley, M. P., Barry, R. A., Braunfeld, M. B., McColloch, J. R. & Prusiner, S. B. (1985) *Cell* **41**, 221–235.
16. Halverson, K., Fraser, P. E., Kirschner, D. A. & Lansbury, P. T., Jr. (1990) *Biochemistry* **29**, 2639–2644.
17. Baker, H. F., Poulter, M., Crow, T. J., Frith, C. D., Lofthouse, R. & Ridley, R. M. (1991) *Lancet* **337**, 1286.
18. Collinge, J., Palmer, M. S. & Dryden, A. J. (1991) *Lancet* **337**, 1441–1442.
19. Palmer, M. S., Dryden, A. J., Hughes, J. T. & Collinge, J. (1991) *Nature (London)* **352**, 340–342.
20. Asakura, S., Eguchi, G. & Iino, T. (1964) *J. Mol. Biol.* **10**, 42–56.
21. Beaven, G. H., Gratzer, W. B. & Davies, H. G. (1969) *Eur. J. Biochem.* **11**, 37–42.
22. Colon, W. & Kelly, J. W. (1992) *Biochemistry* **31**, 8654–8660.
23. Hofrichter, J., Ross, P. D. & Eaton, W. A. (1974) *Proc. Natl. Acad. Sci. USA* **71**, 4864–4868.
24. Jarrett, J. T. & Lansbury, P. T., Jr. (1992) *Biochemistry* **31**, 12345–12352.
25. Chou, P. Y. & Fasman, G. D. (1974) *Biochemistry* **13**, 222–245.
26. Smith, P. K., Krohn, R. I., Hermanson, G. T., Mallia, A. K., Gartner, F. H., Provenzano, M. D., Fujimoto, E. K., Goeke, N. M., Olson, B. J. & Klenk, D. C. (1985) *Anal. Biochem.* **150**, 76–85.
27. Lansbury, P. T. (1992) *Biochemistry* **31**, 6865–6870.
28. Caughey, B. W., Dong, A., Bhat, K. S., Ernst, D., Hayes, S. F. & Caughey, W. S. (1991) *Biochemistry* **30**, 7672–7680.
29. Caughey, B. & Race, R. E. (1992) *J. Neurochem.* **59**, 768–771.
30. Maggio, J. E., Stimson, E. R., Ghilardi, J. R., Allen, C. J., Dahl, C. E., Whitcomb, D. C., Vigna, S. R., Vinters, H. V., Labenski, M. E. & Manyth, P. W. (1992) *Proc. Natl. Acad. Sci. USA* **89**, 5462–5466.
31. Baker, H. F. & Ridley, R. M. (1992) *Neurodegeneration* **1**, 3–16.
32. Griffith, J. S. (1967) *Nature (London)* **215**, 1043–1044.
33. Weissmann, C. (1991) *Nature (London)* **352**, 679–683.
34. Weissmann, C. (1991) *Nature (London)* **349**, 569–571.
35. Hsiao, K. K., Scott, M., Foster, D., Groth, D. F., DeArmond, S. J. & Prusiner, S. B. (1990) *Science* **250**, 1587–1590.
36. Gabizon, R., McKinley, M. P., Groth, D. F., Kenaga, L. & Prusiner, S. B. (1988) *J. Biol. Chem.* **263**, 4950–4955.
37. Asakura, S. (1968) *J. Mol. Biol.* **35**, 237–239.
38. Caspar, D. L. D. (1980) *Biophys. J.* **32**, 101–135.
39. Spencer, R. G. S., Halverson, K. J., Auger, M., McDermott, A., Griffin, R. G. & Lansbury, P. T., Jr. (1991) *Biochemistry* **30**, 10382–10387.
40. Gasset, M., Baldwin, M. A., Lloyd, D. H., Gabriel, J.-M., Holtzman, D. M., Cohen, F., Fletterick, R. & Prusiner, S. B. (1992) *Proc. Natl. Acad. Sci. USA* **89**, 10940–10944.